SPIE Proceedings **3797,** *26, (1999).*

Influence of the Molecular Geometry on the Photoexcitations of Highly Emissive Organic Semiconductors

Shu-Chun Yang[a], Willi Graupner[b*], Suchismita Guha[c], Peter Puschnig[e], Chris Martin[a], H. R. Chandrasekhar[a], Meera Chandrasekhar[a], Günther Leising[d], Claudia Ambrosch-Draxl[e]

[a]*Department of Physics and Astronomy, University of Missouri, Columbia, MO 65211*

[b]*Department of Physics, Virginia Tech, Blacksburg, VA 24061-0435*

[c]*Department of Physics, Marquette University, Milwaukee, WI 53201-1881*

[d]*Institut für Festkörperphysik, Technische Universität Graz, Graz, A 8010 Austria*

[e]*Institut für Theoretische Physik, Universität Graz, Graz, A 8010 Austria*

ABSTRACT

Para-phenylene type molecules are efficient photoluminescence emitters in the ultraviolet-blue-green spectral range. They are used in light emitting diodes (LEDs) and photopumped lasers. Photoexcited *para*-phenylene type molecules give rise to strong emission from singlet excitons, bleaching of the singlet exciton absorption, induced absorption from triplet excitons and induced absorption from polarons. Since the latter two processes represent absorption of the emitted light of singlet excitons, the presence of polarons and triplet excitons might be a fundamental problem for laser diodes made from *para*-phenylene type molecules. In our experiments we modify the molecular geometry by the application of hydrostatic pressures up to 80 kbar in a temperature range of 10 to 300 K. In particular we show how triplet and polaron states, which are present in LEDs under operation, react to the induced geometric changes. The spectra of ground state absorption, excited state emission, bleaching of the singlet exciton absorption, induced absorption from triplet excitons and induced absorption from polarons are significantly broadened and shifted in energy. In order to explain the observed behavior we have performed three-dimensional bandstructure calculations within density functional theory for the planar poly(*para*-phenylene). By varying the intermolecular distances and the length of the polymer repeat unit pressure effects can be simulated.

Keywords: conjugated polymers, high pressure, density functional theory

1. INTRODUCTION

Conjugated polymers have become highly interesting for basic research after the first successful doping of polyacetylene[1] and have been used commercially since 1989[2]. Isolated conjugated molecules are low dimensional electronic systems. However in the solid state, the electronic properties of these materials do substantially depend on three-dimensional interactions (see [3,4] and refs. therein). In principle three-dimensional interactions can either lead to completely new transitions due to collective states such as aggregates (see references in [4]) or to shifts of the energy levels of single molecules due to changes in the molecular geometry such as planarization[5].

In this study we focus on the electronic properties of a methylated laddertype poly(*para*-phenylene) (m-LPPP), which is shown in Figure 2. m-LPPP is a conjugated polymer which has a very low defect content[6], a high PL quantum yield of 30 % in film and 100 % in toluene solution and is used for blue and white light emitting devices[7] and photopumped lasers[8]. Moreover the small inhomogeneous broadening of the emission and absorption spectra in this material enables us to use these spectra as an easily detectable fingerprint for the involved states. All essential electronic states and transitions associated with these states can be monitored either by emission or absorption. Hence we use a phase sensitive photomodulation technique to obtain the spectra of the transitions and the lifetime of the involved species.

In Figure 1 we show a scheme of the electronic states and transitions in conjugated molecules such as m-LPPP. Absorption of light from the singlet ground state S_0 occurs via the creation of a singlet excited state S_1. After photoexcitation de-excitation can occur via several mechanisms including: Nonradiative recombination (NR) leading to a depopulation of S_1

via creation of phonons. Radiative recombination of S_1 leading to photoluminescence (PL). Population of the lowest lying triplet state T_1 via intersystem crossing (ISC) from S_1, which can be probed by triplet-triplet absorption (TT). Dissociation of the S_1 (=bound electron-hole-pair) into a free electron hole pair which creates one positive and one negative polaron, giving rise to intra-polaron absorption (P). Population of triplet and polaron states leading to a small depopulation of the ground state, giving rise to a bleaching of the absorption (PB).

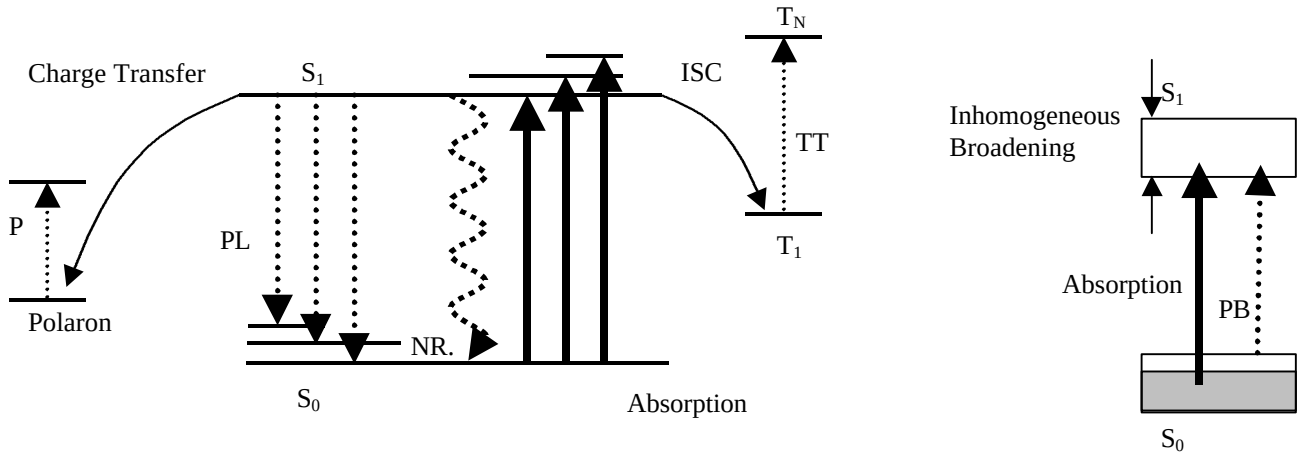

Figure 1: Left: Scheme of electronic states and transitions in conjugated molecules such as m-LPPP. Right: the depopulation of the ground state S_0 can lead to a photobleaching (PB) of the absorption – the width of the photobleaching spectrum depends on the amount of the inhomogeneous broadening in the material.

The application of hydrostatic pressure compresses the lattice, leading to an increased intermolecular interaction and changes in the molecular geometry. In order to model the intermolecular interaction theoretically we have performed three-dimensional (3D) bandstructure calculations within the framework of density functional theory (DFT)[9]. Our computations assume 3D periodicity of the structure hence the solutions of the Kohn-Sham equations are Bloch waves. In that respect our method differs significantly from the quantum chemical approach used in [3,4]: We are able to investigate the influence of intermolecular interactions in an extended 3D system. Within our approach the wave functions are Bloch waves which excludes the description of localized states such as polarons or triplets.

2. METHODOLOGY

2.1. Experimental

The m-LPPP powder (see Figure 2) was provided by U. Scherf and K. Müllen from the MPI for Polymerforschung – the synthesis is described in [10]. A diamond anvil cell (DAC) with a stainless steel gasket was used for hydrostatic pressure studies. Argon was used as the pressure transmitting fluid in the DAC and the luminescence of a ruby chip located in the pressure chamber as pressure calibrant. The pressure range of the work was from 0 to 80 kbar. The films used in the experiments were made by drop-casting a toluene solution of m-LPPP directly onto the bottom diamond surface of the DAC. We studied as prepared and photo-oxidized m-LPPP films. Photo-oxidation was achieved by illuminating the film with 50 mW of the 351.1 nm UV line of an Ar-ion laser for about 8 minutes in air. The photomodulation spectra were taken with the pressure cell in an optical access cryostat at 80 K. The 457.9 nm line of an Ar-ion laser was the pump beam which was modulated by a chopper wheel at frequencies of 10 to 400 Hz. A halogen lamp was used as the probe beam, which passed through the sample and was then dispersed by a SPEX 1702 single stage monochromator. The probe beam was detected with silicon and InGaAs photovoltaic detectors with built-in preamplifiers. Their signal was picked up by a Stanford Research SR 510 lock-in amplifier referenced to the frequency of the chopper wheel. All data shown for the photomodulation are the change of transmission, ΔT, divided by the transmission, T, in order to eliminate the influence of

the probe beam-intensity. Absorption spectra were taken at room-temperature by dividing the sample transmission by the transmission of the empty diamond cell. Photoluminescence spectra were taken by a high resolution double grating SPEX 1401 monochromator with a water cooled high-voltage photomultiplier tube containing a GaAs dynode as the detector. The 351.1 nm ultraviolet line of an argon-ion laser was used to excite the m-LPPP films.

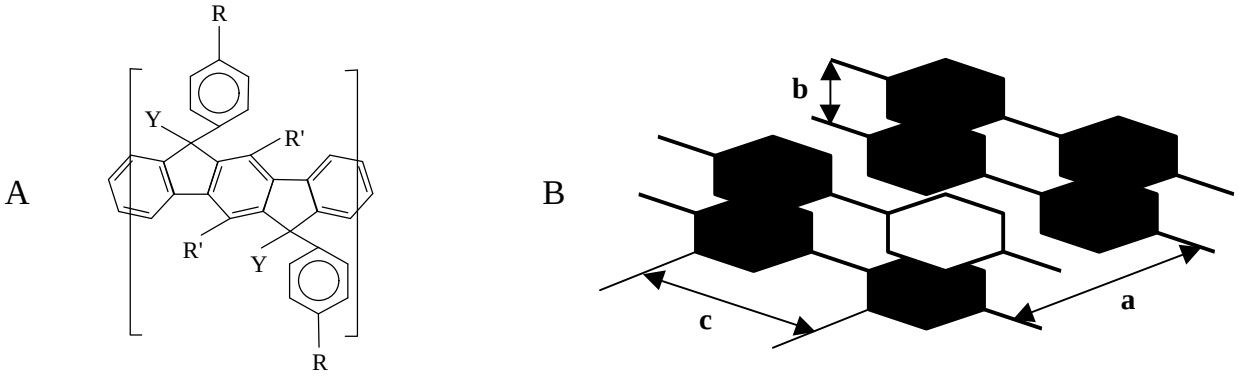

Figure 2: A – left: Chemical structure of the methylated laddertype poly(*para*-phenylene) (m-LPPP) – R=Decyl, R‘=Hexyl, Y=Methyl. The degree of polymerization or length of the polymer is equivalent to 50 phenyl rings. B – right: Three-dimensional arrangement of planar poly(*para*-phenylene) molecules – as used for the bandstructure calculation. The distances a,b,c denote the separation of the chains *in plane* and *perpendicular to the plane* and the length of the *polymer repeat unit* respectively.

2.2. Theory

DFT is a scheme that reduces the calculation of ground state (GS) properties of systems with interacting particles to the solution of single-particle Schrödinger equations (*Kohn-Sham equations*). Their self-consistent solution yields GS properties - such as total energies, electron densities, equilibrium geometries and phonon frequencies. Moreover, the interpretation of the eigenvalues in terms of band structure has been proven successfully for a huge number of solids. For a review of the formalism of DFT as well as high accuracy results for a large number of materials see[11] and references herein. Thus, also quantities involving excited states - such as the dielectric tensor, optical conductivity or optical absorption - can be handled ab-initio. The calculations in this work have been performed for three-dimensional (3D) periodic structures. We have performed 3D bandstructure calculations within DFT for the planar PPP as depicted in Figure 2 B. By varying the intermolecular distances (a,b) as well as the polymer repeat unit (c) pressure effects can be simulated, where the second derivative of the total energy with respect to the lattice constants can be related to the compressibility of the system under pressure. All calculations have been carried out with the full-potential linearized augmented plane wave (FP-LAPW) method utilizing the WIEN97 code[12]. For exchange and correlation effects the generalized gradient approximation according to Perdew et al. has been applied[13]. Optical properties are obtained from an ab-initio computation of the dielectric function (DF): from the knowledge of the single-particle orbitals and energies approximated by the solutions of the Kohn-Sham equation, the DF is calculated. The energies of the conduction bands are corrected according to the scissors operator approximation. For details about the calculation of the DF within the FP-LAPW method see for example[14].

3. RESULTS

In Figure 3 we show the absorption and photoluminescence emission spectra of an m-LPPP film due to singlet exciton transitions, as well as the photoinduced absorption and photobleaching spectra due to triplet-triplet absorption and a bleaching of the ground state singlet exciton absorption. The zero and one phonon vibronic transitions (0-0 and 0-1, respectively) are observed in both PL and absorption. The two phonon 0-2 transition is observed in PL in the low pressure region. The energy levels and different states giving rise to these transitions are described in Figure 1. In the following paragraphs we will describe how all these spectra evolve under pressure.

3.1. Absorption and Emission Spectra Under Pressure

Figure 4 shows the evolution of both absorption and photoluminescence emission spectra of an m-LPPP film with increasing pressure. We find that the 0-2 photoluminescence peak is poorly defined beyond ~30 kbar, and the 0-1

photoluminescence peak is clearly defined only up to ~60 kbar. For both spectra a red shift and broadening of the individual peaks is observed. In order to quantify this behavior we plot the position of the 0-0 and the 0-1 photoluminescence peaks as well as the lowest absorption peak in Figure 5. The rates of shift of the 0-0 and 0-1 photoluminescence peaks are comparable (–2.47 meV/kbar for the 0-0 peak and –2.08 meV/kbar for the 0-1 peak). One striking difference between absorption and photoluminescence peaks is the highly nonlinear pressure-dependence of the absorption in contrast to the linear behavior of the emission as for example observed in polythiophene[15]. This can also be seen from Figure 4: the largest shift of the LPPP absorption occurs at low pressures. The strong broadening of the individual peaks makes the determination of the positions difficult for increasing pressures. This may be the reason that the 0-0 and 0-1 photoluminescence peaks shift by a slightly different rate. Furthermore we note that the absorption edge shifts linearly with pressure as reported in [20].

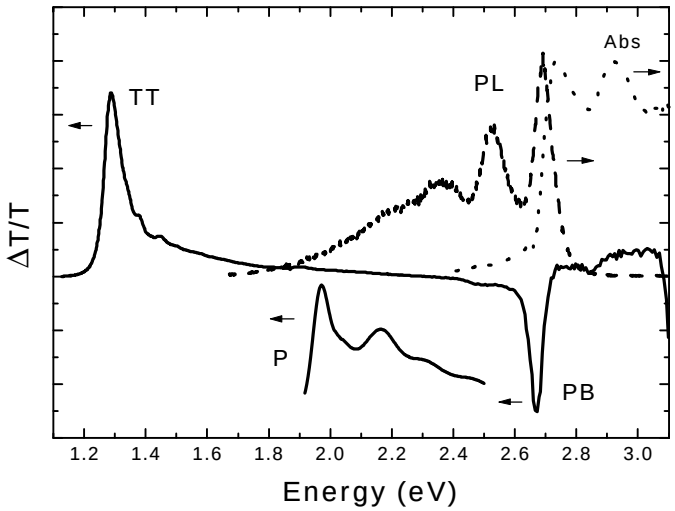

Figure 3: Absorption (Abs, dotted), photoluminescence emission (PL, dashed), photoinduced absorption (TT, solid) and photobleaching (PB, solid) spectra of m-LPPP at 1 bar. The photomodulation spectrum (TT, PB) was taken at 90 K - all other spectra were taken at room temperature. The polaron peak (P, solid) was taken from a doped m-LPPP film and corresponds to what is observed in photoinduced absorption spectra of defect-rich m-LPPP.

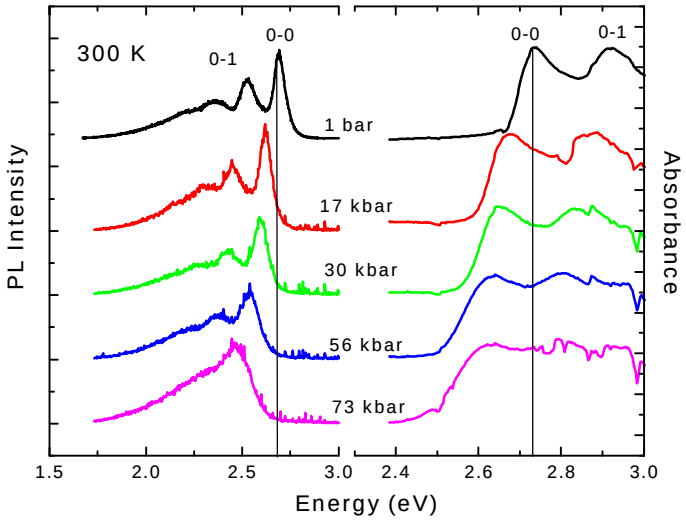

Figure 4: Absorbance (right) and photoluminescence emission (left) spectra of an as-prepared m-LPPP film at room temperature at various pressure values.

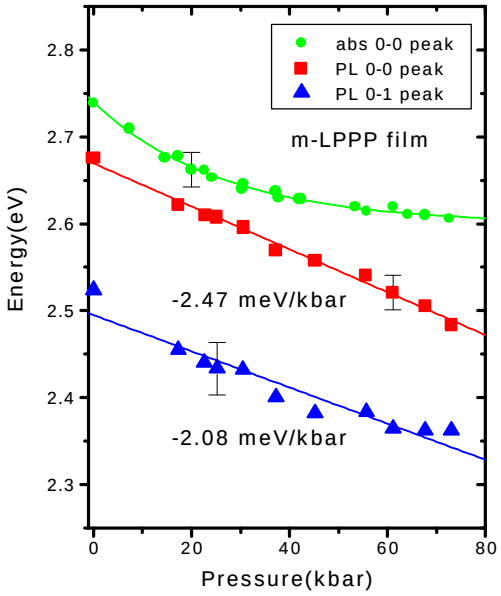

Figure 5: Evolution of the 0-0 absorption peak (circle), the 0-0 and 0-1 photoluminescence emission peaks (square and triangle respectively) of an as-prepared m-LPPP film at room temperature versus pressure.

3.2. Photomodulation Spectra Under Pressure

In Figure 6 we show the photomodulation spectrum of an as-prepared m-LPPP film at 80 K at various pressures. TT-absorption and PB are observed in the spectrum. Both signals shift to lower energy and broaden with increasing pressure. Furthermore the amplitude of the TT-absorption relative to PB decreases. No signatures of polarons are found. This is taken as an indication for a low defect content, like in improved PPV[16], since polarons are stabilized by chemical defects.

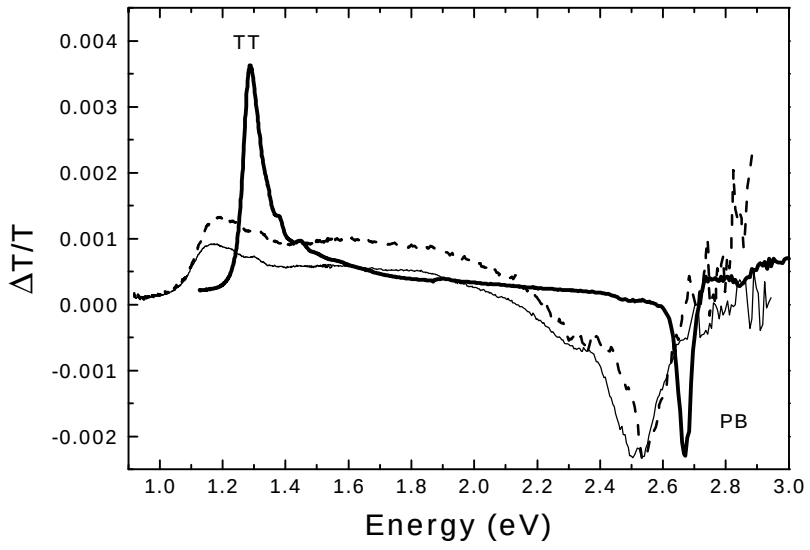

Figure 6: Photomodulation spectra of an as-prepared m-LPPP film for 60 (dashed) and 76 (thin solid) kbar. The chopper frequency was at 145 Hz, the sample temperature at 80 K. The thick solid line represents the 1 bar data as presented in Figure 3.

One way to introduce defects is to photo-oxidize the m-LPPP. This was done for a m-LPPP film and the results are shown in Figure 7. The polaron transition as well as TT and PB are all observed at lower pressure. The polaron peak disappears at high pressures. A red-shift and broadening of the individual peaks are observed with increasing pressure.

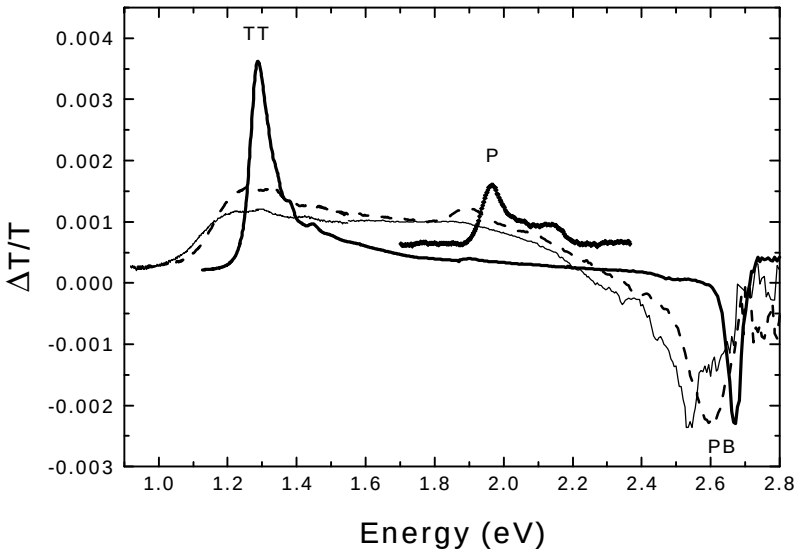

Figure 7: Photomodulation spectra of photo-oxidized m-LPPP for 38 (dashed) and 66 (thin solid) kbar. The thick solid lines represent the 1 bar data as presented in Figure 3. The chopper frequency was at 145 Hz, the sample temperature at 80 K.

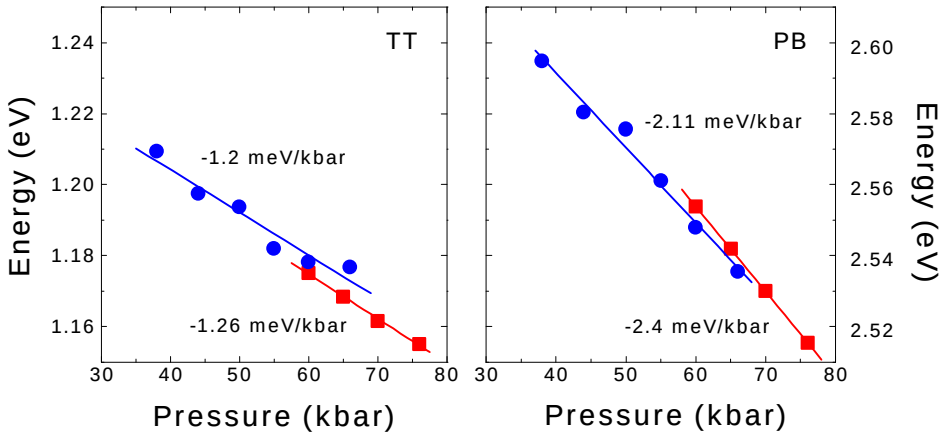

Figure 8: Change of the energetic positon of the triplet-triplet absorption (left) and photobleaching (right) as the pressure is varied. The circles denote the photo-oxidized sample, the squares represent the data for the pure, as prepared sample.

In order to describe the behavior of the TT and PB under pressure, the photomodulation spectrum of the as-prepared and the photo-oxidized m-LPPP films are fitted by Gaussian curves, and the energetic positions of both peaks as a function of pressure are plotted in Figure 8. The linewidths of the peaks increase with pressure. In both m-LPPP films TT and PB showed a red shift with increasing pressure, however they shift at different rates. The rates of the shift of the PB and TT for the as-prepared film are –2.4 meV/kbar and –1.26 meV/kbar, respectively. The rates of the shift of the PB and TT for the photo-oxidized film are –2.11 meV/kbar and –1.2 meV/kbar, respectively. The rates of shift of the PB under pressure for both m-LPPP films are very close to the shift rate of the PL of as-prepared film discussed in Section 3.1 (–2.47 meV/kbar for 0-0 vibronic peak). Because the PB is related to absorption, the shift rates of PB and 0-0 PL peak of the as-prepared m-LPPP film should be very similar, which is verified in our experiments. TheTT-absorption shifts by a smaller rate than the PB for either the as-prepared or photo-oxidized films. Theoretical calculations have shown that the singlet-singlet transition and TT-transition shifted to lower energy when the chain length of the molecules became shorter, and the shift rate of the TT-transition was smaller than the shift rate of singlet-singlet transition when the chain length of the molecule was changed because the triplet states are more localized[17]. Therefore, our result is consistent with the theoretical prediction.

3.3 Lifetimes of the Photoinduced Spectral Features Under Pressure

The lifetimes of the photoinduced spectral features are on the order of a few milliseconds. Thus the dependence of spectral features on the modulation frequency can be used to determine the time constants or lifetimes associated with the species which gives rise to the particular features. In Figure 9 we show the dependence of the photobleaching and the triplet triplet absorption on the frequency of the mechanical chopper. According to our measurements, we find the intensity of the TT and PB to change at the same rate as a function of chopping frequency. This indicates that the TT and PB decrease at the same rate with increasing chopping frequency, and that the chopping frequency used would not affect the relative intensity of these peaks. We discuss these results in Section 4.3.

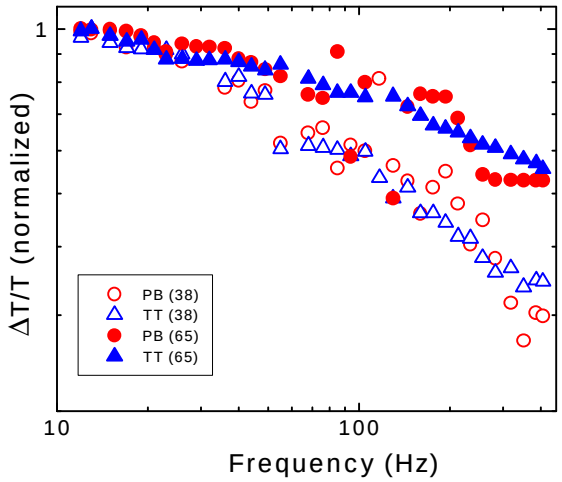

Figure 9: Photobleaching (empty circle) and triplet triplet (empty triangle) signal at 38 kbar and photobleaching (full circle) and triplet triplet (full triangle) signal at 65 kbar versus chopper frequency. The data have been renormalized to yield a value of unity when extrapolated to chopper frequency = 0.

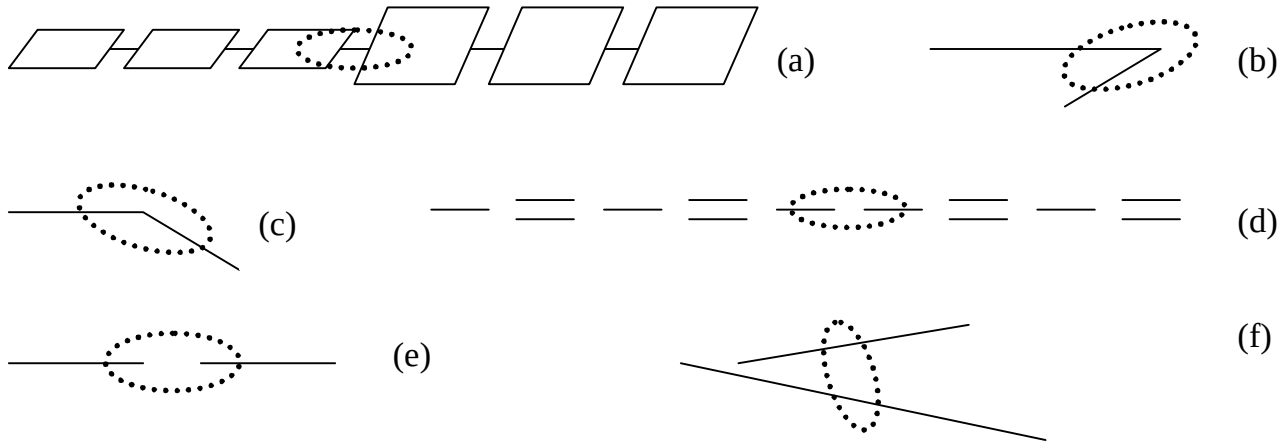

Figure 10: "Defects" which stabilize polarons. (a) torsion of two neighboring units around a single bond, a bent arrangement of the polymer such as an (b) ortho or (c) meta substitution, (d) an interruption of the alternating sequence of single and double bonds, (e) any chain end or (f) interaction with another neighboring chain. The polaron pair is symbolized by the dotted ellipses.

4. DISCUSSION

4.1. Defects in Conjugated Molecules

Any perturbation of the regular periodic one dimensional arrangement of building blocks of a polymer can be seen as a defect. This includes a torsion of two neighboring units around a single bond, a bent arrangement of the polymer such as an ortho or meta substitution on an otherwise *para*-substituted polymer. Furthermore an interruption of the alternating

sequence of single and double bonds, any chain end or even interaction with another neighboring chain is a defect. The previous situations, giving rise to a polaron formation, are illustrated in Figure 10. All these defects have one feature in common: they separate two conjugated segments from each other by an energy barrier and can therefore stabilize the permanent formation of a charge transfer state such as a polaron pair formed by the dissociation of a singlet exciton [18]. The polarons can either overcome these barriers if thermally excited and recombine: the photoinduced absorption due to them disappears[6]. They also can overcome the Coulomb binding if thermally excited and give rise to thermally stimulated currents[6]. It is observed for nearly defect free conjugated molecules that the polaron absorption peaks are not seen in quasi steady state spectroscopy due to the lack of defect induced stabilization[16,19].

In order to detect photoinduced absorption due to polarons we had to photo-oxidize the sample. Figure 11 shows the photoluminescence and the absorption spectra of a m-LPPP film before and after photo-oxidiaztion. The intensity of the 0-0 peak in both the spectra decreases after photo-oxidization, which is an indication of successful introduction of defects in the material.

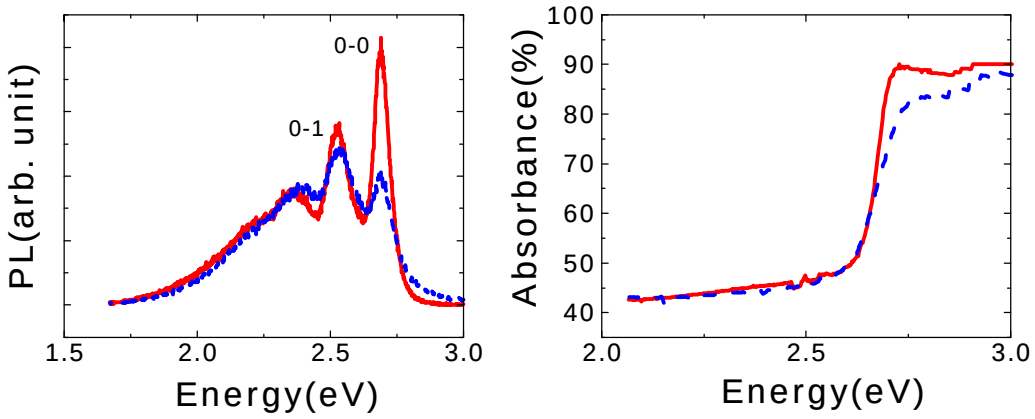

Figure 11: Photoluminescence emission spectrum (left) and absorbance (right) of the m-LPPP film before (solid line) and after (dotted line) photo-oxidation.

4.2. Spectral Evolution of the Spectra Under Pressure

The universal effects observed for all the transitions we have investigate are a broadening and a redshift with increasing pressure. These effects are seen in PL, absorption, and photobleaching, and involve ground- and excited state related vibronics of polarons, singlets and triplets.

In Figure 12 (c) the photoluminescence emission and photobleaching spectra of the m-LPPP film at various cell pressures are shown. The 0-0 photoluminescence peak is at the same energy position as the photobleaching at all pressure points. Both spectra shift to lower energy and are broadened with increasing pressure.

In Table 1 we summarize the shift of the energies related to singlet-singlet transitions under pressure monitored from different optical spectroscopies. All spectra are fitted by Gaussian curves. The linear pressure coefficients, α, of the PL emission and photomodulation spectroscopy are comparable. However, the value obtained from the absorption spectra is much larger than the values obtained from the other experiments. The shift rate quoted here is that of the peak position. For absorption the broadening effect is much stronger than it is for the other spectra. For pressure higher than 50 kbar it is very difficult to get a clear, well resolved of the absorption spectrum.

The α-values obtained in this study can be compared to earlier data of 7.7 meV/kbar and 8 meV/kbar for absorption and photoluminescence respectively[20]. The values of 7.7 meV/kbar and 8 meV/kbar were obtained in a pressure region of 0 - 2 kbar and represent therefore the “initial response“ of the m-LPPP to pressure. From this comparison we conclude that the initially very strong effect of pressure on the electronic properties either saturates or is qualitiatively different at the higher pressure reached in the present study. One possible explanation is the fact that different geometrical changes are associated with different compressibilities and also different changes in the electronic properties. In Ref. [5] we have described how molecular planarity is reached in para-hexaphenyl under high pressure, a nonplanar oligomer of m-LPPP with torsional

degrees of freedom between the phenyl rings. In this case planarization is reached within a range of a few 10 kbars. In the next paragraphs and Figure 12 we show how qualitatively and quantitatively different changes in intra- and intermolecular geometry can lead to very similar changes in the dielectric function.

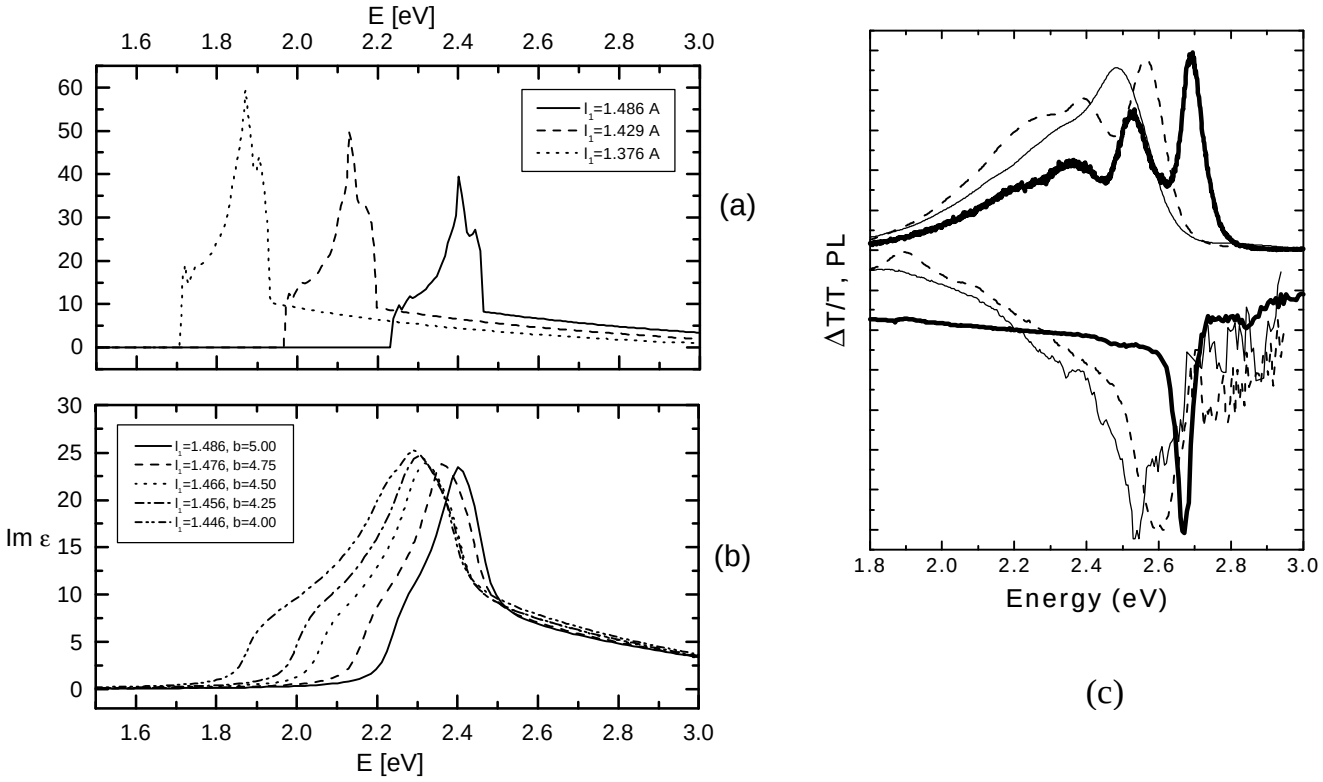

Figure 12: (a) Imaginary part of the dielectric function (Im ε) as calculated for the three dimensional arrangement in Figure 2 B. From left to right we show Im ε for different lengths of the single bond between the phenyl rings: l_1 = 1.376, 1.429, 1.486 Å; (b) Im ε for different $l_1$and b (Figure 2 B), from left to right: (l_1, b) = (1.446 Å, 4.00 Å), (1.456 Å, 4.25 Å), (1.466 Å, 4.50 Å), (1.476 Å, 4.75 Å), (1.486 Å, 5.00 Å); (c) details of Figures 4 and 7, showing the photoluminescence and photobleaching spectra of the m-LPPP film at 38 (dashed) and 66 (thin solid) kbar. The thick solid lines represent the 1 bar data. The noise in the photomodulation spectra at around 2.71 eV is due to the pump-laser.

Table 1: Pressure dependence of absorption, emission and photoinduced absorption spectra as obtained in this work and in pressure studies up to 2 kbar in Ref.[20]. The parameters refer to the following representation of the transition energies: $E = E(0) + \alpha P + \beta P^2$, with P beomg the pressure. Except for the 0-0 Absorption of the as-prepared film studied in this work (Fig. 5) we have set all 0-0 β-values to zero since the linearregression yielded satisfactory results.

Transition	E(0) [eV]	α [meV/kbar]	β [meV/kbar^2]
0-0 PL peak of as-prepared film	2.671 ± 0.003	–2.47 ± 0.07	
0-1 PL peak of as-prepared film	2.495 ± 0.009	–2.08 ± 0.21	
0-0 and 0-1 PL peak of as-prepared film, [20]		8	
0-0 Absorption of as-prepared film	2.732 ± 0.004	–3.78 ± 0.21	0.029 ± 0.003
0-0 Absorption edge of as-prepared film, [20]		7.7	
PB of as-prepared m-LPPP film		–2.40 ± 0.01	
PB of photo-oxidized m-LPPP film		–2.11 ± 0.14	

In order to simulate pressure effects we have varied the in-plane interchain distance **a** as well as the perpendicular distance between two chains **b** and the total length of the chains. The geometrical changes were chosen in such a way to create equilvalently strong shifts in the calculated (Im ε) spectra in Figures 12 (a) and (b). When the length of the chains alone is decreased we find a red shift of the imaginary part of the dielectric function without any broadening as depicted in Fig. 12 (a). However, we find, that a reduction in **a** as well as in **b** only results in a slight blue shift of the absorption peak but mainly leads to a broadening, where the effect is much stronger for the decrease of **b**. The latter effects, the blue-shift as well as the broadening, are due to intermolecular interactions that result in an increased bandwidth of the localized valence and conduction bands. That is, the stronger overlap of the wave functions on two neighboring chains due to decreasing interchain distance results in a higher dispersion of the bands in direction of the interaction and the joint density of states for the optical transition is broadened.

In addition to changing the interchain distances we have also investigated the effects of changing the length of the polymer repeat unit. For each lattice constant c, the bond lengths and angles are relaxed via ab initio force calculations. From the total energy as a function of the lattice constant, we compute the bulk modulus B to be $3*10^{11}$ N/m^2 in good agreement with experimentally reported values[21]. The analysis of the dielectric functions shows that the absorption edge shifts linearly to lower energies upon decreasing the length of the polymer repeat unit. The red-shifted energy gap is simply a result of the increasing bandwidth of the delocalized valence and conduction bands along the polymer axis when the inter-ring bond is decreased. The width of the absorption, however, remains almost constant, because the main contributions to the dielectric function arise from the flat regions in reciprocal space perpendicular to the polymer axis (high joint density of states) which remain unaltered.

Consequently, the experimentally observed red-shift and the broadening of the absorption spectra of m-LPPP under high pressure can be understood, when combining both mechanisms described above. Pressure results in reduced interchain distances causing the broadening as well as in shortend interring bonds shifting the absorption to the red. From the calculated bulk modulus we computed a red-shift of -2.1 meV per kbar, which is close to the experimental value.

4.3. Lifetimes of the Excited States

The influence of a time-constant or lifetime τ on the signal vector $\vec{R}$ measured in a typical optical modulation measurement with a lock in amplifier can be described in the following manner:

$$\vec{R} = \frac{\vec{c}\left\{\exp\left[i\tan^{-1}(2pft)\right]\right\}}{\sqrt{1+(2pft)^2}} \text{ if} \qquad (1)$$

a single time-constant or lifetime is involved. If two time-constants are involved their influence on the signal vector is described by the following equation:

$$\vec{R} = \frac{\vec{c}_1\left\{\exp\left[i\tan^{-1}(2pft_1)\right]\right\}}{\sqrt{1+(2pft_1)^2}} + \frac{\vec{c}_2\left\{\exp\left[i\tan^{-1}(2pft_2)\right]\right\}}{\sqrt{1+(2pft_2)^2}} \qquad (2)$$

where $\vec{R}$ is the intensity of the signal, f is the frequency of the chopper wheel, τ, τ_1 and τ_2 are the lifetimes of the electronic state, and $\vec{c}$, $\vec{c}_1$ and $\vec{c}_2$ represent the weight of each component. $\vec{R}$ has to be written in vector form since it describes both the intensity and the phase of the signal relative to the excitation, i.e in our case the modulated laser pump beam. If there are two time-constants involved it means that there is an initial branching in the population into two separate *uncoupled* states, which decay with different decay rates. If the decay takes place from the same state the decay rates will just add up to $k_{total} = k_1 + k_2$ with the "lifetime" to be $1/\tau_{total} = 1/\tau_1 + 1/\tau_2$. The physical meaning is that there is no single state with one lifetime but there are uncoupled states with different lifetimes.

The optical modulation experiments probe the strength of an electronic transition of states with certain lifetimes. We have used the previous equations to model the measured strength of the electronic transition depending on the frequency of the chopper wheel. As plotted in Figure 9, we have measured (ΔT/T) of the photo-oxidized m-LPPP film for the TT and PB signal at various chopping frequencies at 38 and 65 kbar. We found that the TT and PB signal show a nearly identical behavior. This supports the conclusion that the electrons and holes *populating* the triplet states and therefore creating the

TT signal are the same which *de-populate* the ground state of the sample and give rise to the PB signal. In other words, there are no different states, unaccessible to our experiment, which have to be taken into account since the dynamics of PB and TT are identical.

The data could only be modeled properly by using two time-constants, which are listed in Table 2. The behavior observed is consistent with a weak dependence of the PB and TT signal on chopper frequency. This corresponds to an overall decrease in lifetimes upon increasing the pressure. This is expressed both as a decrease of the lifetimes obtained from the model and as an increase in the weights of the smaller time constants for both transitions. Since smaller lifetimes correspond to less stable states we conclude that the increase in intermolecular interaction destabilizes localized states such as triplets and polarons, as theoretically predicted in [22].

Table 2: Timeconstants as extracted from the data in Figure 9, for the model see equation (2).

Transition	1st timeconstant (ms)	Weight	2nd timeconstant (ms)	Weight
TT (38 kbar)	4.0 ± 0.4	0.61 ± 0.025	0.44 ± 0.07	0.40 ± 0.03
PB (38 kbar)	7.0 ± 2.5	0.48 ± 0.07	0.79 ± 0.10	0.60 ± 0.06
TT (65 kbar)	4.3 ± 0.6	0.28 ± 0.02	0.38 ± 0.03	0.71 ± 0.02
PB (65 kbar)	4.1 ± 1.6	0.34 ± 0.06	0.40 ± 0.10	0.68 ± 0.07

5. CONCLUSIONS

In conclusion, we have shown both experimentally and theoretically how intermolecular interactions influence the electronic properties of a highly fluorescent polymeric organic semicoductor. The photoluminescence emission spectra as well as the singlet exciton ground state absorption, the photobleaching of the ground state absorption, the polaronic and the triplet absorption are all affected by pressure. Qualitatively the picture is similar for all of them – the quantitative changes are different. This can be understood as pressure affecting different states in a different way since the geometries of the neutral ground state, neutral excited states and charged excited states are different. From the investigation about the lifetimes of the excited states we conclude that the photobleaching is completely due to a population of the long living T_1 triplet state and conclude that the increase in intermolecular interaction destabilizes localized states such as triplets and polarons, as theoretically predicted in [22].

ACKNOWLEDGEMENTS

We are indebted to U. Scherf and K. Müllen for the donation of the polymer powder. This work was supported by the University of Missouri Research Board and the Austrian National Bank project 6608. The calculations were carried out with the vector-computer facilites of the University of Graz..

REFERENCES

[1] C. K. Chiang, C. R. Fincher, Y. W. Park, A. J. Heeger, H. Shirakawa, E. J. Louis, S. C. Gau, Alan G. MacDiarmid, "Electrical conductivity in doped polyacetylene, " *Phys. Rev. Lett*. **39**, pp. 1098-1101, 1977.

[2] For a review see e.g.: S. Roth, W. Graupner, P. McNeillis, "Survey of Industrial Applications of Conducting Polymers," *Acta Physica Polonica* **87**, pp. 699-711, 1995; J. S. Miller, "Conducting Polymers – Materials of Commerce", *Adv. Mater*.**5**, pp. 587-589, 1993

[3] J. Cornil, A. J. Heeger, J. L. Bredas, "Effects of Intermolecular Interactions on the Lowest Excited State in Lumincescent Conjugated Polymers and Oligomers," *Chem. Phys. Lett.* **272**, pp. 463-470, 1997.

[4] J. Cornil, D. A. dos Santos, X. Crispin, R. Silbey, J. L. Bredas, "Influence of Interchain Interactions on the Absorption and Lumincescence of Conjugated Oligomers and Polymers: A Quantum-Chemical Characterization,"*J. Am. Chem. Soc.* **120**, pp. 1289-1299, 1998.

[5] S. Guha, W. Graupner, M. Chandrasekhar, H. R. Chandrasekhar, R. Resel, G. Leising, R. Glaser, "On the Planarity of Hexaphenyl," *Phys. Rev. Lett.* **82**, pp. 3625-3628, 1999.

[6] W. Graupner, G. Leditzky, G. Leising, U. Scherf, "Shallow and Deep Traps in Conjugated Polymers of High Intrachain Order," *Phys. Rev. B* **54**, pp. 7610-7613, 1996.

[7] S.Tasch, A.Niko, G.Leising, U.Scherf, "Highly efficient electroluminescence of new wide band gap ladder-type poly(*para*-phenylenes)," *Appl. Phys. Lett.* **68**, pp. 1090, 1996; S. Tasch, J. W. E. List, O. Ekström, W. Graupner, G. Leising, P. Schlichting, U. Rohr, Y. Geerts, U. Scherf, K. Müllen, "Efficient White Light-Emitting Diodes Realized With New Processible Blends of Conjugated Polymers," *Appl. Phys. Lett.* **71**, pp. 2883-2885, 1997.

[8] S. Stagira, M. Zavelani-Rossi, M. Nisoli, S. DeSilvestri, G. Lanzani, C. Zenz, P. Mataloni, G. Leising, "Single-mode picosecond blue laser emission from a solid conjugated polymer ," *Appl. Phys. Lett.* **73**, pp. 2860-2862, 1998.

[9] P. Hohenberg, W. Kohn, "Inhomogeneous Electron Gas," *Phys. Rev.* **136**, pp. 864, 1964; W. Kohn, L. J. Sham, "Self-Consistent Equations Including Exchange and Correlation Effects," *Phys. Rev.* **140**, pp. A1133, 1965.

[10] U. Scherf, K. Müllen, "Polyarylenes and Poly(Arylenevinylenes) - A Soluble Ladder Polymer Via Bridging of Functionalized Poly(Para-Phenylene)-Precursors, *Makromol. Chem., Rapid Commun.* **12**, pp. 489-497, 1991.

[11] R. O. Jones, and O. Gunnarsson, "The density functional formalism, its applictions and prospects", *Rev. Mod. Phys.* **61**, pp. 689, 1989

[12] P. Blaha, K. Schwarz, and J. Luitz, „WIEN97, A Full Potential Linearized Augmented Plane Wave Package for Calculating Crystal Properties", Karlheinz Schwarz, Techn. Universität Wien, Austria, ISBN 3-9501031-0-4, 1999

[13] J. P. Perdew, S. Burke, and M. Enzerhof, "Generalized gradient approximation made simple", *Phys. Rev. Lett.* **77**, pp. 3865-3868, 1996

[14] C. Ambrosch-Draxl, J. A. Majewski, P. Vogl, and G. Leising, „First-Principles Studies of the Structural and Optical Properties of Crystalline Poly(para-phenylene)", *Phys. Rev.* **B** 51, pp. 9668, 1995

[15] B. C. Hess, G. S. Kanner, Z. Vardeny, "Photoexcitations in polythiophene at high pressure," *Phys. Rev. B* **47**, pp. 1407-1411 (1993).

[16] K. Pichler, D. A. Halliday, D. D. C. Bradley, R. H. Friend, P. L. Burn, A. B. Holmes, "Photoinduced Absorption of Structurally Improved Poly(P-Phenylene Vinylene) – No Evidence For Bipolarons", *Synth. Met*. **55**, pp. 230, 1993.

[17] D.Beljonne, J. Cornil, R. H. Friend, R. A. J. Janssen, J. L. Brédas, "Influence of Chain Length and Derivatization on the Lowest Singlet and Triplet States and Intersystem Crossing in Oligothiophenes," *J. Am. Chem. Soc.* **118**, 6453-6461, 1996; J. Cornil, D. Beljenne, J. L. Brédas, "Nature of Optical Transitions in Conjugated Oligomers. II. Theoretical Characterization of Neutral and Doped Oligothiophenes," *J. Chem. Phys.* **103**, pp. 842-849, 1995.

[18] W. Graupner, G. Cerullo, M. Nisoli, S. De Silvestri, G. Lanzani, E. J. W. List, G. Leising, U. Scherf, "Direct Observation of Ultrafast Field-Induced Charge Generation in Ladder-Type Poly(*Para*-Phenylene)," *Phys. Rev. Lett*. **81**, pp. 3259-3262, 1998.

[19] W. Graupner, S. Eder, M. Mauri, G. Leising, U. Scherf, "Excited States in PPP-Type Ladderpolymers Probed by Photoinduced Absorption," *Synth. Met.* **69**, pp. 419-422, 1995.

[20] W. Graupner, S. Eder, K. Petritsch, G. Leising, U. Scherf, "Origin and Stabilization of Photoexcitations in Conjugated Polymers, " *Synth. Met.* **84**, pp. 507-510, 1997.

[21] Landolt-Börnstein Physikalisch-Chemische Tabellen

[22] P. Vogl, D. K. Campbell, "Three-dimensional structure and intrinsic defects in *trans*-polyacetylene," *Phys. Rev. Lett.* **62**, pp. 2012-2015, 1989.